Vasoactive intestinal peptide/vasoactive intestinal peptide receptor relative expression in salivary glands as one endogenous modulator of acinar cell apoptosis in a murine model of Sjögren's syndrome

V. Hauk, M. Calafat, L. Larocca,
L. Fraccaroli, E. Grasso, R. Ramhorst
and C. Pérez Leirós

*Laboratorio de Inmunofarmacología.
Departamento de Química Biológica, Facultad de
Ciencias Exactas y Naturales, Universidad de
Buenos Aires – CONICET, Buenos Aires, Argentina*

Summary

Sjögren's syndrome (SS) is a chronic autoimmune disease characterized by a progressive oral and ocular dryness that correlates poorly with the autoimmune damage of the glands. It has been proposed that a loss of homeostatic equilibrium in the glands is partly responsible for salivary dysfunction with acinar cells involved actively in the pathogenesis of SS. The non-obese diabetic (NOD) mouse model of Sjögren's syndrome develops secretory dysfunction and early loss of glandular homeostatic mechanisms, with mild infiltration of the glands. Based on the vasodilator, prosecretory and trophic effects of the vasoactive intestinal peptide (VIP) on acini as well as its anti-inflammatory properties we hypothesized that the local expression of VIP/vasoactive intestinal peptide receptor (VPAC) system in salivary glands could have a role in acinar cell apoptosis and macrophage function thus influencing gland homeostasis. Here we show a progressive decline of VIP expression in submandibular glands of NOD mice with no changes in VPAC receptor expression compared with normal mice. The deep loss of endogenous VIP was associated with a loss of acinar cells through apoptotic mechanisms that could be induced further by tumour necrosis factor (TNF)-α and reversed by VIP through a cyclic adenosine-5′-monophosphate (cAMP)/protein kinase A (PKA)-mediated pathway. The clearance of apoptotic acinar cells by macrophages was impaired for NOD macrophages but a shift from inflammatory to regulatory phenotype was induced in macrophages during phagocytosis of apoptotic acinar cells. These results support that the decline in endogenous VIP/VPAC local levels might influence the survival/apoptosis intracellular set point in NOD acinar cells and their clearance, thus contributing to gland homeostasis loss.

Keywords: acinar cell apoptosis and clearance, Sjögren's syndrome, VIP

Introduction

Sjögren's syndrome (SS) is a chronic autoimmune disease with a prevalence of 0·3–0·5% in adults that affects mainly women, in a 9 : 1 relationship [1–4]. The hallmark of SS is a progressive oral and ocular dryness that correlates poorly with the focal infiltration, within large areas of morphologically intact parenchyma, found in salivary gland biopsies. It has been proposed that a loss of homeostatic equilibrium in the glands is partly responsible for salivary dysfunction which would, in turn, increase the susceptibility of the glands to the autoimmune attack [3–6]. In line with this, labial

biopsies and acinar cell primary cultures from SS patients show an aberrant expression and activation of inflammatory mediators in epithelial cells together with defective activity and localization of key enzymes and channels involved in saliva secretion [5–8]. This observation supports the hypothesis that acinar cells are involved actively in the pathogenesis of SS and provides new evidence to the search of early biomarkers for diagnosis and/or disease activity. At the prediabetic stage, the non-obese diabetic (NOD) mouse model of Sjögren's syndrome has the unique characteristic of developing a deep secretory dysfunction with mild infiltration of the glands [9–11] consistent with a structural–dysfunctional

aetiology. In keeping with this, early neurotransmitter receptor-signalling alterations have been reported in NOD females' submandibular glands unrelated to the onset of the autoimmune response [12–14]. Among them, a progressive loss of activity of the neural isoform of nitric oxide synthase (NOS 1) in NOD exocrine glands at the Sjögren's syndrome-like period has been described [12,15]. The lower levels of NOS activity were found in glands of 16-week-old NOD mice that presented increased apoptosis of acinar cells and increased levels of tumour necrosis factor (TNF)-α, among other T helper type 1 (Th1) cytokines in the serum [15,16]. Vasoactive intestinal peptide (VIP), described initially as a vasodilator and prosecretory neuropeptide, has trophic effects on acini [17,18] and strong anti-inflammatory properties in several models of chronic inflammatory diseases [19–21]. Prediabetic NOD mice treated systemically with VIP showed increased serum interleukin (IL)-10 and reduced Th1 cytokine levels [22] while gene-transfer of VIP onto NOD submandibular glands prevented saliva secretion loss and partly reduced glandular Th1 cytokine expression [23]. Furthermore, VIP showed a clear anti-apoptotic effect on acinar cells isolated from NOD submandibular glands driven to apoptosis through TNF-α/TNF-αR1-mediated pathways [16].

An adequate balance of apoptosis of epithelial cells and their silent clearance by professional phagocytes is central for gland homeostasis. On this basis, we hypothesized that the local expression of VIP/VPAC system could modulate acinar cell apoptosis and clearance, thus influencing gland homeostasis. We present evidence on a progressive decline of VIP expression in submandibular glands of NOD mice that encompasses a loss of acinar cells through apoptotic mechanisms. We also show that apoptotic acinar cells are removed by NOD macrophages with a reduced phagocytic efficacy compared to control macrophages, although in a suppressor manner that is stabilized by VIP.

Materials and methods

Animals

NOD and BALB/c female mice were bred and maintained in the Central Animal Care facility at the School of Exact and Natural Sciences, University of Buenos Aires. They were tested routinely for blood glucose levels and considered prediabetic, as their values of serum glucose on two occasions over a 24-h period did not differ significantly from those of control mice (0.9 ± 0.1 g/l, $n = 42$). NOD mice of 16 weeks of age used in this study presented a reduced saliva flow rate (>35% reduction) compared with BALB/c control mice. Studies were conducted according to standard protocols of the Animal Care and Use Committee of the School of Exact and Natural Sciences, University of Buenos Aires.

Acinar cell and macrophage isolation and cultures

Submandibular glands were removed and transferred immediately to ice-cold RPMI-1640, 10% fetal bovine serum (FBS) for acinar cell isolation, as described previously [16]. Acinar cells were washed and seeded on flat-bottomed 24-well microtitre plates (Corning Glass, Corning, NY, USA) and incubated for 2 h at 37°C in a humidified incubator with 5% CO_2 to separate immune adherent cells and viability determination [16]. When used, recombinant TNF-α (Promega, Madison, WI, USA) (5–10 ng/ml) was added to acinar cell culture for 3·5 h [reverse transcription–polymerase chain reaction (RT–PCR)] or for 6 h (annexin V staining and immunoblotting). In some experiments, cells were preincubated for 30 min with 100 nM VIP (PolyPeptide Labs, Strasbourg, France) before TNF-α addition in the presence or absence of H89 (1 μM). Macrophages were obtained by washing the peritoneal cavity with ice-cold RPMI-1640, as reported [24,25]. Cells were seeded at 5×10^5 cells/well (Corning Glass), incubated at 37°C for 2 h and washed thoroughly before co-cultures, nuclear factor (NF)-κB activation or cytokine determination.

Co-cultures and assessment of phagocytosis and macrophage phenotype

Macrophages were co-cultured with freshly isolated acini or acini previously induced to apoptosis with TNF-α. Incubations were run at 37°C for the times indicated. VIP (100 nM) was added 30 min before the addition of acini. After incubation, acini were removed and macrophages were washed with fresh medium. Haematoxylin and eosin (H&E) staining was used for phagocytosis determination [24]. Cells were collected for cytokine expression by quantitative RT–PCR (qRT–PCR) or flow cytometry analysis; nitrite production was determined by the Griess in supernatants, as described previously [24,25]. For flow cytometry, cells were stained with fluorescein isothiocyanate (FITC)-conjugated anti-F4/80 monoclonal antibody for 30 min (eBioscience, San Diego, CA, USA), fixed in 4% paraformaldehyde/phosphate-buffered saline (PBS)–2% FCS, permeabilized with 0·5% saponin (Sigma, St Louis, MO, USA) and incubated with phycoerythrin (PE)-conjugated anti-IL-10 monoclonal antibody (BD) or with the PE-conjugated immunoglobulin (Ig)G1 isotype; 10 000 events were acquired in a fluorescence activated cell sorter (FACS)Aria cytometer® and results analysed using the WinMDI software®. Cytokines were determined by ELISA and prostaglandin E_2 (PGE_2) by radioimmunoassay (RIA), as described [24,25].

Conventional and real-time RT–PCR

Total RNA was extracted from acinar cells or macrophages with Trizol (Gɪʙᴄᴏ, Carlsbad, CA, USA), as described

[16,24]. Reverse-transcribed cDNAs were amplified using specific primers for VIP, VPAC1, VPAC2, bax, TNF-α and glyceraldehyde-3-phosphate-dehydrogenase (GAPDH) and conditions as stated previously [16,24–27]. The following sequences were used for forward and reverse primers. Bax: 5′-GGAATTCCAAGAAGCTGAGCGAGTGT-3′ and 5′-GGAATTCTTCTTCCA GATGGTGAGCGAG-3′; VPAC1: 5′-GTGAAGACCGGCTACACCAT-3′ and 5′-TGAAGAGG GCCATATCCTTG-3′; VPAC2: 5′-CCAAGTCCACACTGCT GCTA-3′ and 5′-CTCGCCATCTTCTTTTCAG-3′; VIP: 5′-TTCACCAGCGATTACAGCAG-3′ and 5′-TCACAGCCA TTTGCTTTCTG-3′; TNF-α: 5′-CCTTGTTCGGCTCTC TT TTGC-3′ and 5′-AGTGATGTAGCGACAGCCTGG-3′ GAPDH: 5′-TGATGACAT CAAGAAGGTGGTGAAG-3′ and 5′-TCCTTGGAGGCCATGTAGGCCAT-3′. PCR products were size-fractionated on 2% agarose gels and visualized by staining with ethidium bromide using a size molecular marker. For real-time experiments, VIP and TNF-α expression were determined as described [26,27].

NF-κB activation assays

Western blot (WB) assays and confocal microscopy were used to analyse NF-κB activation in acinar cells or macrophages. For WB assays, both cytosolic and nuclear fractions were analysed independently after cell isolation. Isolated cells were washed gently and homogenized in 10 mM HEPES pH 7·9; 1 mM ethylenediamine tetraacetic acid (EDTA); 1 mM ethylene glycol tetraacetic acid (EGTA), 5 mM sodium fluoride (NaF), 1 mM NaVO4, 1 mM dithio-threitol (DTT), 10 mM KCl, 0·5% NP-40 with protease inhibitors, as described [16,24]. After 15 min on ice, samples were centrifuged at 8000 *g* for 15 min. Supernatants (cytosolic extracts) were fractionated in 12% sodium dodecyl sulphate-polyacrylamide gel electrophoresis (SDS-PAGE) gels and immunoblotted with rabbit polyclonal anti-I-κB-α or goat polyclonal anti-actin (Santa Cruz Bio-technology, CA, USA) [24]. Nuclear extracts were obtained by resuspending pellets in 10 mM HEPES pH 7·9, 1 mM EDTA, 1 mM EGTA, 5 mM NaF, 1 mM NaVO4, 10 mM Na2MO4, 1 mM DTT and 0·4 M KCl, 20% glycerol. Proteins were fractioned on 10% SDS-PAGE gels and immunoblotted with anti-p65 or goat polyclonal anti-actin (Santa Cruz Biotechnology) Bands were revealed with peroxidase-conjugated antibodies and enhanced chemiluminescence detection system (Pierce, Rockford, IL, USA). Densitometry analysis of proteins was performed with ImageQuant®. For confocal microscopy studies, acini or macrophages were fixed and permeabilized with methanol at −20°C, incubated with mouse p65 antibody (Santa Cruz Biotechnology) and FITC-conjugated anti-mouse antibody (BD Phar-mingen, San Diego, CA, USA), washed and stained with 0·5 μg/ml propidium iodide (PI) and observed at confocal microscope Olympus FV 300 coupled to Olympus BX61.

Acinar cell apoptosis assays

To study apoptosis of acinar cells WB, RT–PCR and annexin V/propidium iodide staining and cytometric detection were used. For WB, acinar cells were homogenized at 4°C in 50 mM Tris-HCl buffer pH 7·5 with 0·15 % Triton X-100, as reported previously [16]. After centrifugation at 5000 *g* 10 min, supernatants were frozen at −80°C until used. Extracts (50 μg protein/lane) subjected to 10% SDS-PAGE were immunoblotted with antibodies to total Bad, phospho-rylated Bad (Santa Cruz Biotechnology) and revealed by enhanced chemiluminescence (ECL) detection system (Pierce). Densitometric analysis of protein levels was per-formed with ImageQuant software. The frequency of apop-totic acini cells was also assessed by flow cytometry analysis with Annexin V/IP double staining following the manufac-turer's recommendations (BD). Flow cytometry data were acquired in a FACSAria cytometer® and results analysed using WinMDI software®. For bax expression assays, acinar cells were homogenized either freshly or after induction with TNF-α and RT–PCR experiments were carried out as indi-cated above and previously [16].

Statistical analysis

Statistical significance of differences was determined by the two-tailed *t*-test for independent populations. When mul-tiple comparisons were necessary, the Student–Newman–Keuls test was used after analysis of variance. Differences between groups were considered significant at *P* < 0·05.

Results

Expression pattern of VIP/VPAC in NOD mice submandibular glands

Figure 1a shows the expression kinetics of VIP and their receptors in submandibular glands isolated from NOD mice of different ages from postnatal day 2 to 20 weeks of age. Compared to normal mice, NOD mice showed the highest level of VIP expression at 4 weeks of age and decreased thereafter. The progressive decrease in VIP expression from the fourth week takes place with no changes in VPAC1 and VPAC2 receptors. A clear reduction of VIP levels was evident in NOD submandibular glands at 16 weeks of age (Fig. 1a), which was confirmed by qRT–PCR (Fig. 1b). The decline in VIP/VPAC1 relative expression over time is similar to the kinetics of neural nitric oxide synthase (nNOS) activity and salivary secretion loss shown previously [12].

Effect of VIP on apoptosis-prone acinar cells from NOD glands

NF-κB appears as an intracellular pivotal determining factor that conditions the apoptotic or survival fate of TNF-α-
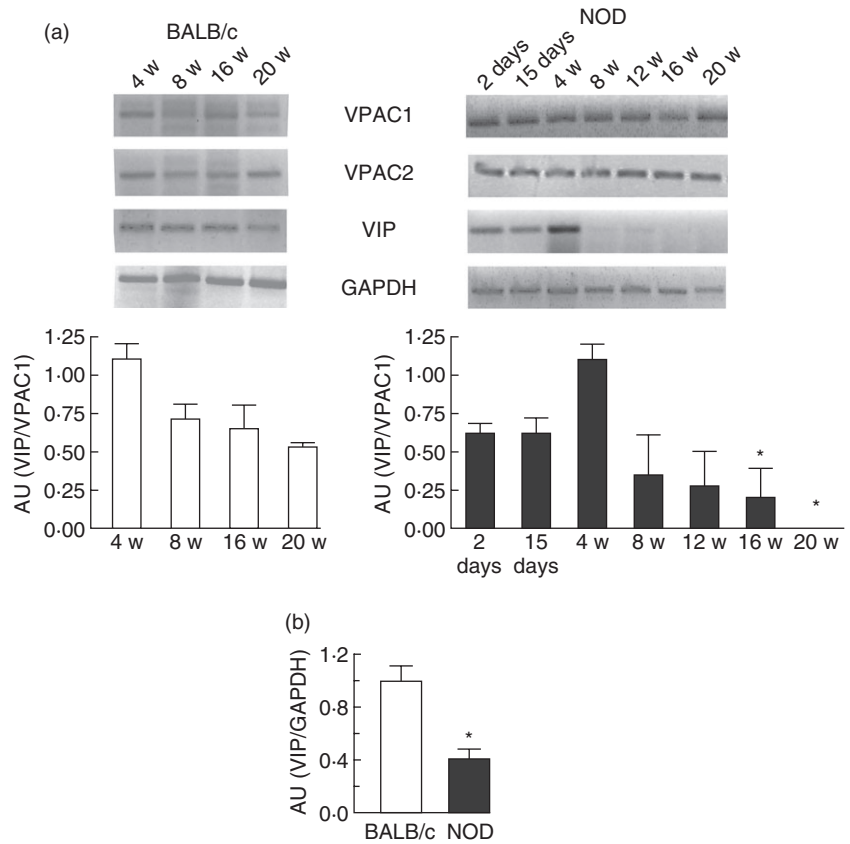
Fig. 1. Vasoactive intestinal peptide/vasoactive intestinal peptide receptor-1(VIP/VPAC1) relative expression in submandibular glands of non-obese diabetic (NOD) mice. Glands from NOD and control BALB/c mice of the ages stated in the figure were excised and processed for VIP, VPAC1 and VPAC2 expression determined by reverse transcription–polymerase chain reaction (RT–PCR) (a) or real-time RT–PCR (b), as indicated in Materials and methods. Gels shown are representative of at least six others carried out for each cDNA. The density of the bands for VIP and VPAC1 obtained in all the assays were plotted as mean ± standard error of the mean (s.e.m.) for either control or NOD glands. *$P < 0.05$ *versus* 4 weeks in NOD glands and 16 weeks in BALB/c.

stimulated cells [28]. Thus, we analysed NF-κB activation and apoptosis in response to TNF-α in NOD acinar cells. As shown in Fig. 2a, acinar cells from NOD glands present a basal translocation of p65 of NF-κB to the nucleus (merge image with PI-stained nuclei) that is not seen in normal BALB/c mice. Consistent with this, WB analysis of I-κB in the cytosolic fraction or p65 in the nuclear fraction revealed that p65 appeared located to the nucleus, while I-κB expression was increased in cytosol of acini in basal conditions (Fig. 2b). Moreover, when treated *in vitro* with TNF-α, NOD mice acinar cells showed an abnormal NF-κB activation kinetics compared with BALB/c acinar cells (Fig. 2a,b). Figure 2c shows that NOD freshly isolated acini were primarily committed to apoptosis and that TNF-α further induced this effect at concentrations that were not effective in control acinar cells, consistent with the higher expression of TNF-αR1 in NOD acini reported previously [16].

To analyse the role of VIP/VPAC system in isolated acinar cells, we determined VIP and VPACs expression. Figure 3a shows that VPAC1 is expressed on acinar cells while VIP and VPAC2 receptor subtypes are not. We assessed that VIP inhibition of bax expression and apoptosis of acinar cells entails the VPAC1/cyclic adenosine-5′-monophosphate (cAMP)/protein kinase A (PKA) signalling pathway involving the phosphorylation of Ser 112 on Bad by PKA, as both VIP-reduced bax expression and Bad phosphorylation were

inhibited with H89 (Fig. 3b). There was no effect of VIP on NF-κB activation in this acinar cell preparation (not shown).

Phagocytosis of apoptotic acinar cells by NOD macrophages

One of the ultimate goals of the apoptotic programme is the silent clearance of apoptotic bodies by phagocytic cells for the maintenance of tissue homeostasis. To analyse the macrophage function in the maintenance of gland homeostasis in NOD mice and the role of VIP, we intended to reconstitute the first steps *in vitro* of the interaction between apoptotic acinar cells and macrophages. Figure 4a shows the rapid morphological changes undergone by NOD macrophages 30 min after addition of apoptotic acinar cells, as well as the phagocytic function of NOD and control macrophages. Figure 4a also shows a lower phagocytic function of NOD macrophages compared with control cells which was not modified by VIP. The phagocytic defect of NOD macrophages could be determined with acinar cells induced or not to apoptosis with TNF-α, remaining at the lowest levels detectable in either condition (Fig. 4a). In the case of BALB/c, phagocytosis was only assayed with TNF-α-induced apoptotic acini. We then analysed the phenotypic profile of NOD and BALB/c peritoneal macrophages before and after interaction with homologous apoptotic acinar cells. Figure 4b
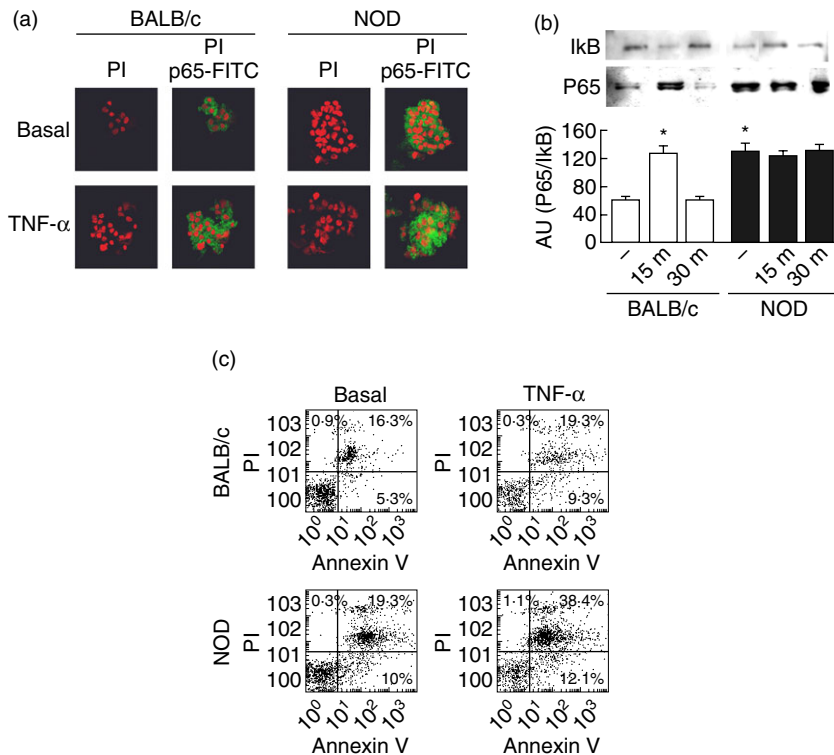
Fig. 2. Nuclear factor (NF)-κB activation and apoptosis in non-obese diabetic (NOD) acinar cells. (a) Acinar cells isolated from 16-week-old NOD and BALB/c submandibular glands were incubated with p65 antibody or propidium iodide for confocal assays, as indicated in Materials and methods. BALB/c and NOD acinar cell cultures were treated for 30 min with tumour necrosis factor (TNF)-α (10 ng/ml) for NF-κB activation before immunofluorescence staining of p65 and merge confocal images were photographed at ×200. Photographs shown are representative of the whole slices in three similar experiments. (b) Immunoblotting assays with anti-p65 or anti I-κB-alpha were performed at the times indicated in the presence or not of 10 ng/ml TNF-α on nuclear (p65) and cytosolic (I-κB) acinar fractions, as described in Materials and methods. Results are mean ± standard error of the mean (s.e.m.) of corresponding band densities of p65/I-κB in arbitrary units of at least three experiments run similarly. *$P < 0.05$ *versus* basal in BALB/c. (c) Annexin V/PI staining and flow cytometry plots of acinar cells in basal conditions and after treating cultures for 6 h with TNF-α (10 ng/ml). Percentages shown on the plots indicate different apoptotic acinar cell populations and represent the results of three similar experiments.

shows that NOD macrophages expressed an inflammatory phenotype in resting conditions revealed by the basal activation of NF-κB (merge image and p65 abnormal levels in cytosol and nucleus), by the higher basal levels of TNF-α, IL-12, nitric oxide (NO) and reduced levels of PGE$_2$. However, when they were faced with apoptotic acinar cells, the inflammatory profile of NOD macrophages was shifted to a regulatory phenotype (Fig. 4c). Regardless of the extent of apoptosis of acinar cell preparations, TNF-α and NO production in NOD macrophages were reduced drastically to normal levels similar to BALB/c macrophages, while IL-10 levels were increased. VIP further stabilized an anti-inflammatory and suppressor phenotype with high IL-10 ($10.7 \pm 0.2\%$ double-positive cells) and low nitrite production to undetectable values (<5 μM).

Discussion

We analysed the expression profile of VIP and its VPAC receptors in submandibular glands of NOD mice from birth throughout the Sjögren's syndrome-like disease period and the effect of the neuropeptide on the apoptosis and clearance of acinar cells isolated from salivary glands. Our results indicate a progressive loss of VIP/VPAC1 relative expression in NOD glands, with the lowest levels observed at 16 weeks of age coincident with an increased apoptosis of NOD acinar cells. VIP/VPAC1 expression did not vary in BALB/c glands with mouse age and, in contrast with NOD glands, freshly isolated acinar cells seemed not to be prone to apoptosis. Acinar cells from NOD mice could be further induced to apoptosis with a concentration of TNF-α (10 ng/ml) that was almost ineffective in normal acinar cells. VIP inhibited TNF-α-induced apoptosis in NOD acinar cells through a VPAC1/cAMP/PKA pathway, while neither VPAC2 receptors nor the neuropeptide could be detected in acini, indicating that their expression in whole glands would not correspond to acinar cells. Finally, we found a reduced phagocytic index of NOD macrophages to engulf apoptotic acinar cells compared to normal macrophages, but their basal inflammatory phenotype was
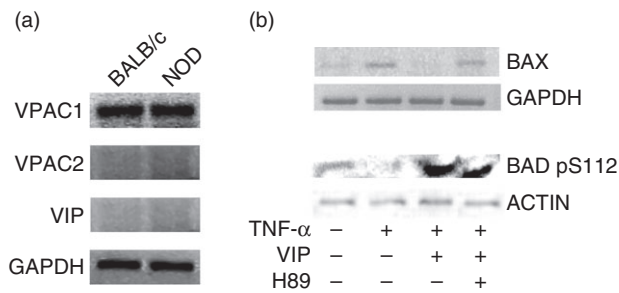
Fig. 3. Vasoactive intestinal peptide/vasoactive intestinal peptide receptor-1(VIP/VPAC1) expression on acinar cells and inhibition of apoptosis, (a) Acinar cell cultures from non-obese diabetic (NOD) and BALB/c mice submandibular glands were homogenized and reverse transcription–polymerase chain reaction (RT–PCR) assays were carried out. (b) Acinar cells isolated from 16-week-old NOD submandibular glands were pretreated with 100 nM VIP before apoptosis was induced with tumour necrosis factor (TNF)-α (10 ng/ml) for 3·5 h in the presence or absence of H89 inhibitor of protein kinase A (PKA) (1 μM) and homogenized for RT–PCR or immunoblotting detection, as described in Materials and methods. Results shown are representative of four other experiments for VIP, VPACs, Bax or Bad carried out similarly.

suppressed during phagocytosis and VIP stabilized this suppressor regulatory phenotype.

It is noteworthy that the time–course of VIP/VPAC1 relative expression decline is similar to the kinetics of nNOS activity loss shown previously and parallels the reduction in the secretory response to muscarinic acetylcholine receptor stimulation [12]. It also coincided with the loss of acinar cell homogeneous structure of the glands and a higher ductal to acinar cell ratio in the glands at 16 weeks of age [12]. The localization of this enzyme is normally confined to neural fibres in close proximity to gland epithelial cells where NO contributes to salivary flow. Consistent with this, NOD mice submandibular glands showed a reduced NOS activation through VIP receptors that coincided with the reduction in salivary flow [15]. While VIP can induce NOS in peripheral and central neurones, VIP expression is regulated by neural NOS activity and knock-out mice for neural NOS isoform express lower neuronal VIP levels [29]. In rat salivary glands VIP is localized in nerve fibres rather than in acinar cells, being mainly released from nerves surrounding acini where it displays trophic effects on epithelial cells [17,18]. In fact, the release of trophic and anti-apoptotic stimuli from nerve terminals with long-term effects on salivary gland parenchyma is the rationale of a newly designed device to restore salivary flow in patients with SS and other *sicca*-associated pathologies [30]. Acinar cells from both normal and NOD submandibular glands express only VPAC1 receptors, as reported previously [16]. In these cells, VIP was able to reduce apoptosis via cAMP/PKA pathway, as derived from the fact that H89 reversed VIP effect on bax expression [16] and Bad phosphorylation, a step previous to the loss of its apoptotic effect through binding to 14–3–3 in cytosol [31].

Evidence shown here indicates that acinar epithelium of NOD but not BALB/c glands present increased apoptosis along with a dysregulated NF-κB basal activation consistent with a predominant apoptosis-to-survival intracellular set-point. This was confirmed when cells were incubated with TNF-α, as this cytokine induced a significant increase of acinar cell apoptosis, but it failed to activate NF-κB in NOD acinar cells, providing new evidence to the role of this nuclear factor in acinar cell fate.

Apoptosis of the secretory epithelium as a triggering factor of early dysfunction and autoimmune response has been explored in SS patients and models [32–34] and the potential of certain TNF-α superfamily members, as SS susceptibility biomarkers has emerged from microarray studies in a transgenic mice model of SS [35]. Remarkably, local over-expression of TNF-αR1 in murine glands was shown to reduce saliva secretion [36], while TNF-α has been reported as a potent inducer of acinar apoptosis and TNF-αR1 expression in prediabetic NOD mice [16]. However, TNF-α/TNF-αR1 effects are also commonly associated with cytokine synthesis and cell survival in immune cells, being the final cellular fate determined primarily by a pivotal factor such as NF-κB [28]. NF-κB is dysregulated in autoimmune disorders and, particularly in SS patients but not in other autoimmune disorders, a lack of a proteasome subunit – multi-functional peptidase 2 – in immune cells could result in a lower NF-κB activity [37].

Finally, macrophage high functional plasticity guarantees the silent clearance of apoptotic cells that involves the synthesis of anti-inflammatory mediators IL-10, PGE$_2$ and TGF-β to maintain tissue homeostasis [38]. While NOD macrophages expressed an inflammatory profile in resting conditions, a shift to a regulatory phenotype of NOD macrophages was seen when faced to apoptotic acinar cells. Interestingly, NOD macrophages presented lower phagocytosis of acinar apoptotic cells. A lower avidity and efficacy to engulf apoptotic thymocytes has been reported previously for NOD macrophages [39–41]. In contrast to results presented herein, phagocytosis of apoptotic thymocytes elicited an inflammatory profile in NOD macrophages, suggesting that selective suppressor mechanisms might be involved in the clearance of apoptotic acinar cells. Evidence presented here also suggests that VIP might contribute to the homeostatic surveillance function of macrophages in the glands by stabilizing a regulatory phenotype for silent phagocytic clearance.

Acknowledgements

Disclosure

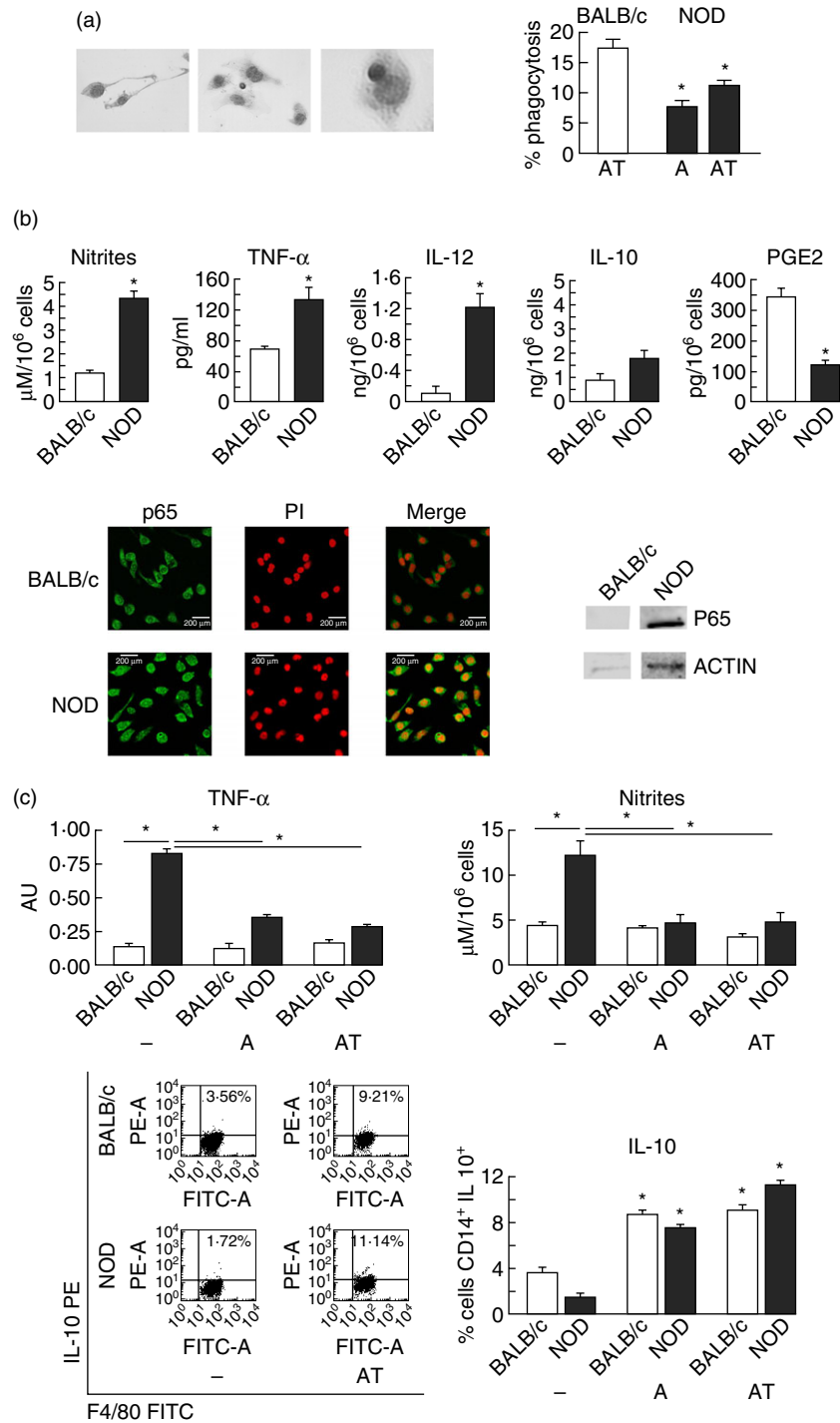The authors declare that they have no competing interests.

Fig. 4. Phagocytosis of apoptotic acinar cells and macrophage phenotype. (a) Photographs of non-obese diabetic (NOD) mice macrophages with morphological changes and engulfing apoptotic cells are shown. Macrophages from NOD and BALB/c mice were incubated for 90 min with homologous apoptotic acinar cells shown as (a) (basal apoptotic acini only available in NOD mice) or tumour necrosis factor (TNF)-α (10 ng/ml)-induced apoptotic acini (AT) for NOD and BALB/c mice. Results are mean ± standard error of the mean (s.e.m.) of four assays and were expressed as % of cells engulfing at least one apoptotic body. *$P < 0.05$ *versus* BALB/c. (b) Macrophage basal synthesis of indicated cytokines, nitrites and prostaglandin E_2 (PGE$_2$) in BALB/c and 16-week-old NOD mice. Bars shown are mean ± s.e.m. of at least three determinations. *$P < 0.05$ *versus* BALB/c. Basal translocation to the nucleus of nuclear factor (NF)-κB p65 as assessed by confocal and immunoblotting assays performed in NOD and BALB/c peritoneal macrophages, as described in Materials and methods. Confocal images were photographed at ×200 as well as immunoblots shown are representative of three similar experiments. (c) NOD and BALB/c macrophages were co-cultured for 90 min with homologous acinar apoptotic cells, and after removal of acini cells were incubated for an additional 12 or 24 h for nitrites, TNF-α and interleukin (IL)-10 determination by Griess, real-time reverse transcription–polymerase chain reaction (RT–PCR) or flow cytometry, as indicated in Materials and methods. For IL-10, cytometry dot-plots show the percentage of IL-10-positive cells inside the electronically gated F4/80-positive population. Results shown are mean ± s.e.m. of at least three assays carried out in similar conditions. *$P < 0.05$ *versus* basal values in BALB/c (IL-10) or *versus* bars compared as indicated.

References

1 Ng WF, Bowman SJ, Griffiths B, on behalf of the UKPSSR study group. United Kingdom Primary Sjögren's Syndrome Registry – a united effort to tackle an orphan rheumatic disease. Rheumatology 2011; **50**:32–9.

2 Gabriel SE, Michaud K. Epidemiological studies in incidence, prevalence, mortality, and comorbidity of the rheumatic diseases. Arthritis Res Ther 2009; **11**:229. doi:10.1186/ar2669. Available at: http://arthritis-research.com/content/11/3/229.

3 Fox RI. Sjögren's syndrome. Lancet 2005; **366**:321–31.

4 Mavragani CP, Moutsopoulos NM, Moutsopoulos HM. The management of Sjögren's syndrome. Nat Clin Pract Rheumatol 2006; **2**:252–2261.

5 Manoussakis MN, Moutsopoulos HM. Sjögren's syndrome: autoimmune epithelitis. Ballière's Clin Rheumatol 2000; **14**:73–95.

6 Konttinen Y, Porola P, Konttinen L, Laine M, Poduval P.

Immunohistopathology of Sjögren's syndrome. Autoimmun Rev 2006; **6**:16–20.

7 Törnwall J, Konttinen YT, Tuominen RK, Törnwall M. Protein kinase C expression in salivary gland acinar epithelial cells in Sjögren's syndrome. Lancet 1997; **349**:1814–51.

8 Steinfeld SD, Appelboom T, Delporte C. Treatment with infliximab restores normal aquaporin 5 distribution in minor salivary glands of patients with Sjögren's syndrome. Arthritis Rheum 2002; **46**:2249–51.

9 van Blokland SC, Versnel MA. Pathogenesis of Sögren's syndrome: characteristics of different mouse models for autoimmune exocrinopathy. Clin Immunol 2002; **103**:111–24.

10 Lee BH, Tudares MA, Nguyen CQ. Sjögren's syndrome: an old tale with a new twist. Arch Immunol Ther Exp (Warsz) 2009; **57**:57–66.

11 Delaleu N, Immervoll H, Cornelius J, Jonsson R. Biomarker profiles in serum and saliva of experimental Sjögren's syndrome: associations with specific autoimmune manifestations. Arthritis Res Ther 2008; **10**:R22.

12 Rosignoli F, Roca V, Meiss R, Leceta J, Gomariz RP, Pérez Leirós C. Defective signalling in salivary glands precedes the autoimmune response in the non-obese diabetic mouse model of sialadenitis. Clin Exp Immunol 2005; **142**:411–18.

13 Jonsson MV, Delaleu N, Brokstad KA, Berggreen E, Skarstein K. Impaired salivary gland function in NOD mice: association with changes in cytokine profile but not with histopathologic changes in the salivary gland. Arthritis Rheum 2006; **54**:2300–5.

14 Berggreen E, Nylokken K, Delaleu N, Hajdaragic-Ibricevic H, Jonsson MV. Impaired vascular responses to parasympathetic nerve stimulation and muscarinic receptor activation in the submandibular gland in non-obese diabetic mice. Arthritis Res Ther 2009; **11**:R18.

15 Rosignoli F, Roca V, Meiss R, Pregi N, Pérez Leirós C. Inhibition of calcium-calmodulin kinase restores nitric oxide production and signaling in submandibular glands of a mouse model of salivary dysfunction. Br J Pharmacol 2004; **143**:1058–65.

16 Calafat M, Larocca L, Roca V *et al.* Vasoactive intestinal peptide inhibits TNF-alpha-induced apoptotic events in acinar cells from nonobese diabetic mice submandibular glands. Arthritis Res Ther 2009; **11**:R53. doi:10.1186/ar2671. Available at: http://arthritis-research.com/content/11/2/R53.

17 Ekström J. Autonomic control of salivary secretion. Proc Finn Dent Soc 1989; **85**:323–31.

18 Månsson B, Nilsson BO, Ekström J. Effects of repeated infusions of substance P and vasoactive intestinal peptide on the weights of salivary glands subjected to atrophying influences in rats. Br J Pharmacol 1990; **101**:853–8.

19 Gomariz RP, Juarranz Y, Abad C, Arranz A, Leceta J, Martinez C. VIP–PACAP system in immunity: new insights for multitarget therapy. Ann NY Acad Sci 2006; **1070**:51–74.

20 Gonzalez-Rey E, Ganea D, Delgado M. Neuropeptides: keeping the balance between pathogen immunity and immune tolerance. Curr Opin Pharmacol 2010; **10**:473–81.

21 Gomariz RP, Gutiérrez-Cañas I, Arranz A *et al.* Peptides targeting Toll-like receptor signalling pathways for novel immune therapeutics. Curr Pharm Des 2010; **16**:1063–80.

22 Rosignoli F, Torroba M, Juarranz Y *et al.* VIP and tolerance induction in autoimmunity. Ann NY Acad Sci 2006; **1070**:525–30.

23 Lodde BM, Mineshiba F, Wang J *et al.* Effect of human vasoactive intestinal peptide gene transfer in a murine model of Sjögren's syndrome. Ann Rheum Dis 2006; **65**:195–200.

24 Larocca L, Hauk V, Calafat M *et al.* Modulation of macrophage inflammatory profile in pregnant nonobese diabetic (NOD) mice. Mol Cell Endocrinol 2011; **333**:112–18.

25 Larocca L, Calafat M, Roca V, Franchi AM, Pérez Leirós C. VIP limits LPS-induced nitric oxide production through IL-10 in NOD mice macrophages. Int Immunopharmacol 2007; **7**:1343–9.

26 Roca V, Larocca L, Calafat M *et al.* Reduced nitric oxide synthase and cyclo-oxygenase activity in the uterus of NOD mice. Reproduction 2006; **132**:931–8.

27 Jimeno R, Gomariz RP, Gutierrez-Cañas I, Martínez C, Juarranz Y, Leceta J. New insights into the role of VIP on the ratio of T-cell subsets during the development of autoimmune diabetes. Immunol Cell Biol 2010; **88**:734–45.

28 Dale E, Davis M, Faustman DL. A role for transcription factor NF-kB in autoimmunity: possible interactions of genes, sex and the immune response. Adv Physiol Educ 2006; **30**:152–8.

29 Kim MJ, Joo KM, Chung YH *et al.* Vasoactive intestinal peptide (VIP) and VIP mRNA decrease in the cerebral cortex of nNOS knock-out(–/–) mice. Brain Res 2003; **978**:233–40.

30 Strietzel FP, Lafaurie GI, Mendoza GR *et al.* Efficacy and safety of an intraoral electrostimulation device for xerostomia relief: a multicenter, randomized trial. Arthritis Rheum 2011; **63**:180–90.

31 Zha J, Harada H, Yang E, Jockel J, Korsmeyer SJ. Serine phosphorylation of death agonist BAD in response to survival factor results in binding to 14-3-3 not BCL-X(L). Cell 1996; **87**:619–28.

32 Kong L, Ogawa N, McGuff HS *et al.* Bcl-2 family expression in salivary glands from patients with primary Sjögren's syndrome: involvement of Bax in salivary gland destruction. Clin Immunol Immunopathol 1998; **88**:133–41.

33 Kong L, Ogawa N, Nakabayashi T *et al.* Fas and Fas ligand expression in the salivary glands of patients with primary Sjögren's syndrome. Arthritis Rheum 1997; **40**:87–97.

34 Kong L, Robinson CP, Peck AB *et al.* Inappropriate apoptosis of salivary and lacrimal gland epithelium of immunodeficient NOD-SCID mice. Clin Exp Rheumatol 1998; **16**:675–81.

35 Nguyen CQ, Cornelius JG, Cooper L *et al.* Identification of possible candidate genes regulating Sjögren's syndrome-associated autoimmunity: a potential role for TNFSF4 in autoimmune exocrinopathy. Arthritis Res Ther 2008; **10**:R137. doi:10.1186/ar2560. Available at: http://arthritis-research.com/content/10/6/R137.

36 Vosters JL, Yin H, Roescher N, Kok MR, Tak PP, Chiorini JA. Local expression of tumor necrosis factor-receptor 1: immunoglobulin G can induce salivary gland dysfunction in a murine model of Sjögren's syndrome. Arthritis Res Ther 2009; **11**:R189.

37 Krause S, Kuckelkorn U, Dörner T, Burmester GR, Feist E, Kloetzel PM. Immunoproteasome subunit LMP2 expression is deregulated in Sjogren's syndrome but not in other autoimmune disorders. Ann Rheum Dis 2006; **65**:1021–7.

38 Mosser DM, Edwards JP. Exploring the full spectrum of macrophage activation. Nat Rev Immunol 2008; **8**:958–69.

39 O'Brien BA, Huang Y, Geng X, Dutz JP, Finegood DT. Phagocytosis of apoptotic cells by macrophages from NOD mice is reduced. Diabetes 2002; **51**:2481–8.

40 Stoffels K, Overbergh L, Giulietti A *et al.* NOD macrophages produce high levels of inflammatory cytokines upon encounter of apoptotic or necrotic cells. J Autoimmun 2004; **23**:9–15.

41 Marée AF, Komba M, Finegood DT, Edelstein-Keshet L. A quantitative comparison of rates of phagocytosis and digestion of apoptotic cells by macrophages from normal (BALB/c) and diabetes-prone (NOD) mice. J Appl Physiol 2008; **104**:157–69.